UNIVERSITAT POLITÈCNICA DE CATALUNYA
BARCELONA**TECH**
Escola d'Enginyeria de Barcelona Est

BACHELOR'S THESIS

Degree in Biomedical Engineering

GENERATION OF HUMAN NEURAL TUBE ORGANOIDS WITHIN A MICROFLUIDIC DEVICE

Report

Author: Carla Juanes Duran
Thesis Supervisor: Adrian Ranga
Mentor: Brian Daza Jimenez
Call: June 2020

Preface

I would like to thank Adrian Ranga for accepting me into the LBM and for giving me the opportunity of living this challenging and exciting semester. I have learned more than I would ever imagine before, thank you for your help. I also want to thank Brian Daza, firstly, to let me join his amazing project and for teaching me. But most importantly, for his sympathy and kindness. I wish you the best. Thank you too to the rest of the GOT, Idris and Aravind, I appreciated a lot this little team. It made work much more enjoyable. I would also like to thank Elena, Katrine, Lorenzo, María and Niko, for the beautiful moments also outside of the laboratory, and to Abdel, Andi, and Sergei, for your friendship and your help. Finally, a lot of love to my family and my friends, for being there even at more than 1200 km of distance.

Carla Juanes Duran

Contents

Abstract

The spinal cord has a modular structure where spinal neurons with the same function occupy the same stereotypical position [1]. This spatial segregation emerges during the early development of the spinal cord, when the neural tube, the embryonic precursor of the central nervous system, patterns in both dorsal-ventral (DV) and anterior-posterior (AP) axis, induced by concentration gradients of morphogens such as sonic hedgehog (Shh) [2]. The patterning of the embryonic spinal cord is a complex process that is being studied by numerous research groups [1][3]–[9]. However, we still lack an *in-vitro* model capable of recapitulating completely and simultaneously the DV and AP patterning, which would be a key to study the human embryonic spinal cord development. One of the projects of the Laboratory of Bioengineering and Morphogenesis (LBM) of the KU Leuven is to develop this model taking advantage of two technologies: organoids culture and microfluidic devices. On one side, organoid technology is a promising tool for this purpose because it allows recapitulating key features of development, such as tissue-specific cell types and its 3D architecture [10]. Moreover, it permits the study of human-specific features in contrast to animal models. On the other side, microfluidic technology allows the generation of high-resolution antiparallel concentration gradients [11] that can mimic the *in-vivo* morphogen gradients involved in the spinal cord patterning [5]. Also, by using 3D printing, its fabrication process becomes flexible, low-cost and simple [11]. In the LBM, it has already been designed a microfluidic device that recreates the Shh morphogen gradient that induces the ventral neural progenitor domains of the embryonic spinal cord, by using smoothened agonist. In this thesis, I biologically characterize the device. To achieve it, firstly, I culture human neural tube organoids within the microfluidic device following an adapted well-established protocol of the LBM [12]. Secondly, I evaluate its health by comparing them with hNTOs cultured in a plate, as a control. During the evaluation, I identify problems related to the timing of the protocol, the design of the microfluidic device, the sterilization process, among others. Finally, I optimize both the protocol and the microfluidic device, and I improve the development and health of the organoids, apart from the robustness and reliability of the *in-vitro* model. Moreover, I propose which would be the next steps to keep working on its development.

List of Figures and Tables

List of Figures

List of Tables

List of Abbreviations

AP	Anterior-posterior
bHLH	Basic-helix-loop-helix
BMP	Bone morphogenic protein
CAD	Computer-aided design
CNS	Central nervous system
DV	Dorsal-ventral
ESC	Embryonic stem cell
FGF	Fibroblast growth factor
Gdf11	Growth differentiation factor 11
GRN	Gene regulatory network
HD	Homeodomain
hNTO	Human neural tube organoid
IN	Interneuron
iPSC	Induced pluripotent stem cell
LBM	Laboratory of Bioengineering and Morphogenesis
micro-HIVE	Microhexagon interlace for generation of versatile and fine gradients
MN	Motor neuron
NP	Neural progenitor
RA	Retinoic acid
RNA	Ribonucleic acid
nd-PEG-A	Non-degradable polyethylene glycol A
SAG	Smoothened agonist
SCO	Spinal cord organoid
Shh	Sonic hedgehog
TF	Transcription factor
3-DiSC	3D spinal cord induction condition

Chapter 1

Background and Objectives

This thesis is part of a bigger project of the Laboratory of Bioengineering and Morphogenesis (LBM), led by Prof. Adrian Ranga, of the KU Leuven.

During my internship, I worked with Brian Daza, a PhD student whose broad objective is to generate human spinal cord organoids (hSCOs) patterned in both dorsal-ventral (DV) and anterior-posterior (AP) axis, taking advantage of the microfluidic device technology. The final aim is to use hSCOs as *in-vitro* models of spinal cord development.

When I arrived, a microfluidic device that allows mimicking *in-vivo* antiparallel gradients of patterning factors had been already designed. Moreover, its fabrication process had been optimized and the gradient formation was being characterized. Thus, the next step was to evaluate the possibility of culturing and patterning organoids inside the microfluidic device, and this was my responsibility.

Specifically, my role was to culture neural tube organoids (hNTOs) following a well-established protocol of the LBM [13] within the predesigned microfluidic device, to evaluate both the protocol and the device, and optimize them to be able to culture and pattern SCOs within the device in a future.

Therefore, my project aimed to:

1) Acquire the skills of a laboratory researcher and learn the protocols of the LBM.

   a. Learn the basics of working in a chemical laboratory.
   b. Learn hiPSC and hNTO culture.
   c. Learn printing techniques for fabricating microfluidic devices.

2) Culture hNTOs inside the microfluidic device.

   a. Adapt the protocol for hNTO culture to make it compatible with the device.
   b. Analise the formed gradient inside the device and adapt it to pattern the hNTOs.

3) Evaluate the development of the hNTOs inside the microfluidic device.

   a. Compare the health between hNTOs cultured in the plate and the device.
   b. Check if the hNTOs are patterned matching the concentrations of patterning factors.

4) Optimize the culturing protocol and the microfluidic device.

   a. Modify the device or the protocol to improve the health and patterning of the hNTOs.
   b. Modify the device or protocol to make the culturing process more robust and reliable.

Chapter 2

Introduction

2.1. Spinal Cord Development and Patterning

The spinal cord is a neural structure located inside the vertebral canal that, together with the brain, forms the central nervous system (CNS) [14].

After analysing the internal organization of the spinal cord, it has been observed that spinal neurons with the same function occupy the same stereotypic position. Thus, the spinal cord has a modular structure where different groups of neuronal populations are distributed along the anterior-posterior (AP) and dorsal-ventral (DV) axis [1].

The position of the pools of motor neurons (MNs) that innervate the limb muscles is an example of this organization. Regarding the DV axis, all the pools are in the ventral spinal cord (

Figure 1 A); and, regarding the AP axis, they are distributed along the cervical or lumbar regions of the spinal cord, depending on their corresponding muscle target (

Figure 1 B) [15].
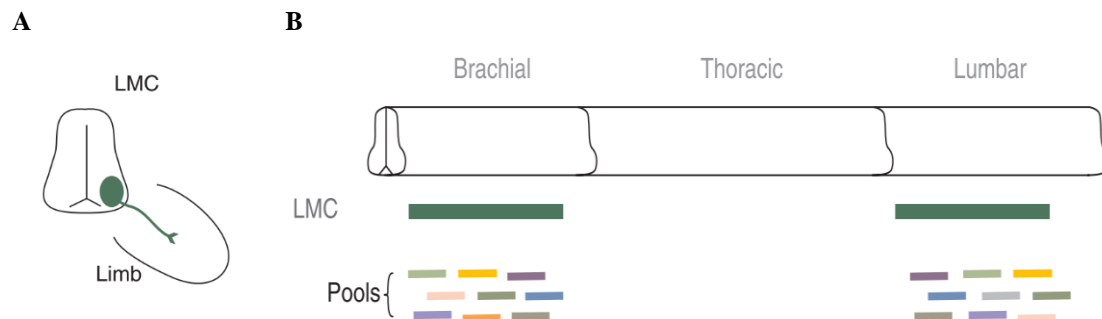
Figure 1.- Position of the lateral motor column (LMC), and its corresponding motor pools along the DV and AP axis of the spinal cord. (A) DV cross-section of the spinal cord, showing the location of the LMC in the ventral region. (B) Location of the LMC and its motor pools along the AP axis of the spinal cord, distributed between the brachial and lumbar regions. Adapted from [15]

It is known that this spatial segregation emerges during the early development of the spinal cord, when the neural tube, the embryonic precursor of the CNS, patterns in both the DV and the AP axis [1]. The neural tube forms during a process called neurulation, in which one region of the ectoderm thickens forming the neural plate (Figure 2 A), that later folds (Figure 2 B, C) and extends giving rise to the neural tube (Figure 2 D) [2].
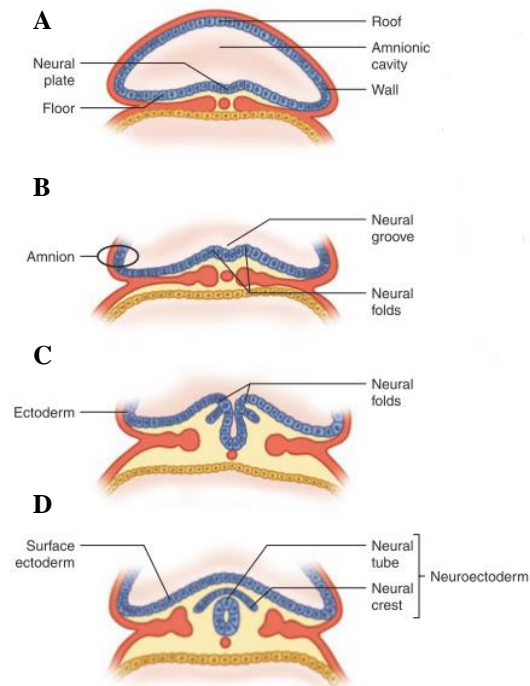
Figure 2.- Cross-sectional diagram of primary neurulation. (A) During days 18-19 post-conception it appears as a thickening in the midline of the ectoderm call neural plate. (B, C) The neural plate invaginates into the body, (D) and separates from the surface ectoderm forming a hollow tube call the neural tube [16].

The patterning of the neural tube occurs during neurulation, due to the effect of a concentration gradient of morphogens [2].

Morphogens are defined as secreted signalling molecules that, by forming concentration gradients, organize a field of surrounding cells into patterns. The concentration gradient starts at a localized source that emanates morphogens and extends by dispersion covering the zone of the generation of the new tissue. At each point of the gradient, the concentration of morphogen gives information about the distance to the source. Thereby, each uncommitted cell perceives its position and adopts accordingly its corresponding arrangement and fate, pattering the tissue [3].

The AP patterning is induced by an antiparallel gradient of the morphogens retinoic acid (RA), fibroblast growth factor (FGF), Wnt families, and growth differentiation factor 11 (Gdf11). The activity of the RA, secreted from the somatic mesoderm, induces the most anterior cell identities of the spinal cord; and FGFs, Wnt, and Gdf11, produced by the tail bud, promote the posterior identities. The AP axis is patterned in neural progenitor (NP) domains which identities are conferred by the expression of a family of TF encoded by the Hox genes. Hox 4-7 genes define the cervical region of the spinal cord, Hox 9 the thoracic and Hox 10-11 the lumbar (Figure 3) [7][1].

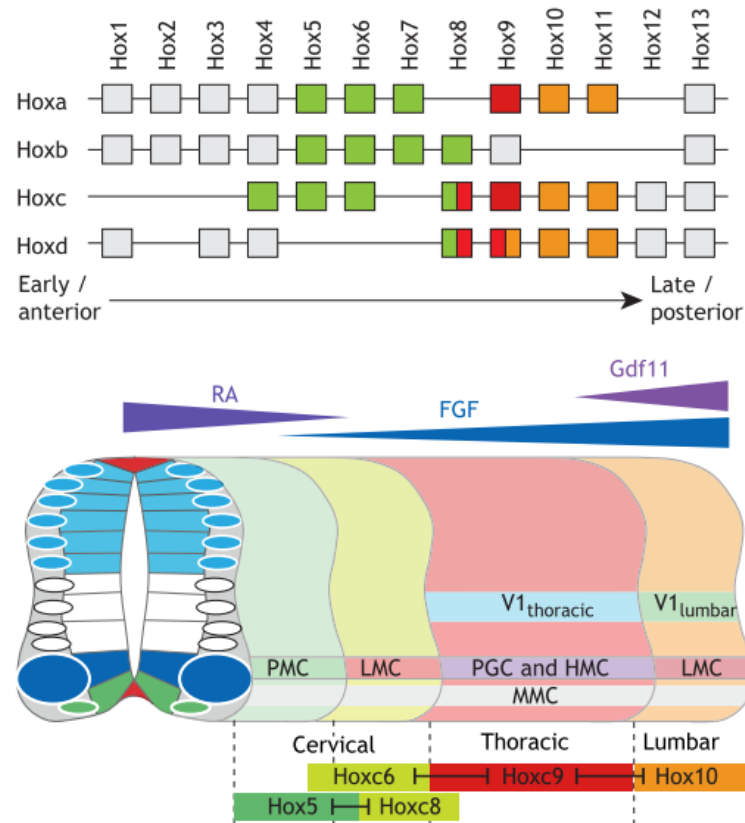**Figure 3.- Patterning along the AP axis of the embryonic spinal cord.** An antiparallel concentration gradient of morphogens induces a patterning in the AP axis in the spinal cord based, which is based on different cell expression of the Hox gens. The four Hox gene clusters (a, b, c, d) and the 13 groups (Hox1, Hox2, Hox3, etc.) are shown above. They are painted in different colours depending on where they are expressed. Green, red, and orange correspond to the cervical, thoracic, and lumbar regions respectively [1].

Along the DV axis, the neural tube is patterned by an antiparallel gradient of the morphogen sonic hedgehog (Shh), the bone morphogenetic protein (BMP) and the Wnt families. Shh, which is secreted at the beginning from the notochord and later from the floor plate, induces the identity of five ventral NP domains, p0, p1, pMN and p3. BMP and Wnt families, produced by the roof plate, and later also by some dorsal NP, establishes six dorsal progenitor identities, which are pd1 to pd6. These morphogens act by inducing different expression of the TFs basic-helix-loop-helix (bHLH) domain and homeodomain (HD) along the DV axis. As these TFs are expressed in discrete but overlapping regions, the distinct NP domains can be determined depending on their combination of bHLH and HD. For example, the TF profile of the pMN domain includes the bHLH protein Olig2 and the HD factors Pax6 and Nkx6.1 [1][17].

Each NP domain gives rise to a different type of neurons. The NP domains from dp4 to dp6 differentiate into five association interneuron (IN) subtypes: initially dI3 to dI6, and later dILA and dILB. In the case of dp1 to dp3 NP, the generated INs are dV1 to dV3. Finally, the pMN give rise to MN. After their generation, each type of neurons expresses a set of TFs. For example, MNs express Mnx1, Isl1, Lhx3 and Isl2 (Figure 4) [6].
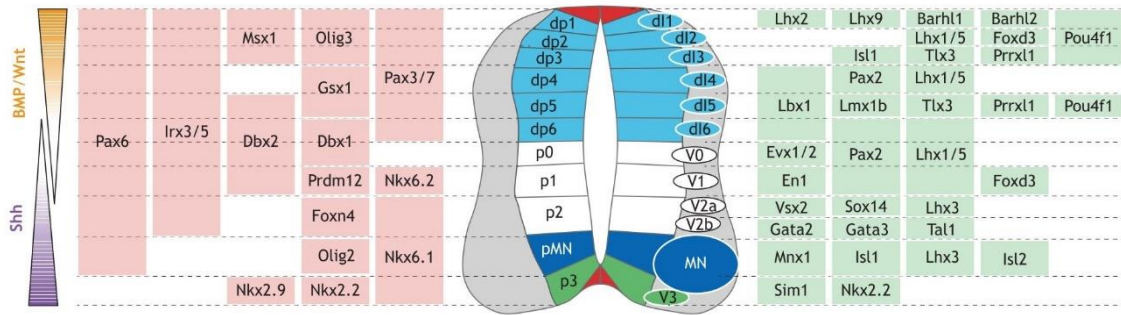
Figure 4.- Transversal section of an AP patterned embryonic spinal cord. In the left, the antiparallel gradient of the morphogens Shh and BMP/Wnt is shown. Then, in pink, the TF expressed by the distinct NP domains. In the middle, the NP domains, and the neuronal subtypes given rise by each NP. Finally, in the right, in green, the expression of TFs that characterize the neuronal subtypes [1].

The formation of NP and neuronal subtypes in the spinal cord also varies depending on the time. This temporal variation of the patterning is primarily controlled by the gene regulatory network (GRN), which is an architecture of relations between different TFs involved in the patterning of the spinal cord, in a way that the TFs are cross-regulated between them. One example of cross-regulation is the relation between the TFs Olig2, Nkx2.2, Pax6 and Irx3. Due to the GRN, not only the levels of morphogens acts as an input for patterning but also the duration of its exposition [1].
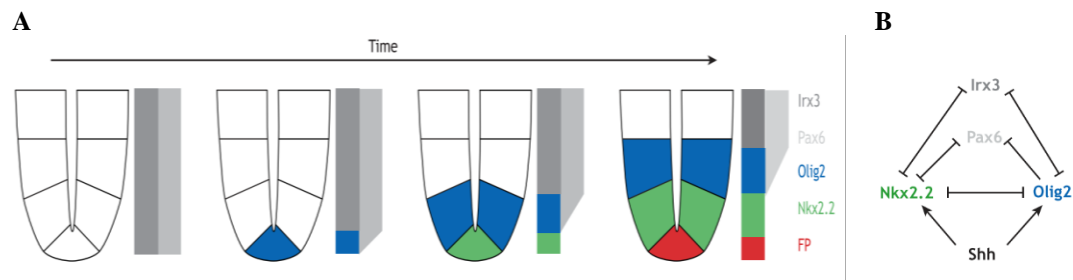
Figure 5.- Induction overtime of the ventral spinal cord NP domains. (A) First, the NP domains express Irx3 and Pax6. Later, Olig2 and Nkx2.2 are sequentially induced, due to an increase of the duration and level of Shh. (B) The GRN controlling the sequential induction of the TFs Olig2, Nkx2.2, Pax6, and Irx3 and its relationship with Shh [1].

2.2. In Vitro Model of Spinal Cord Development

The patterning of the embryonic spinal cord is a complex process, that is being studied by numerous research groups [1][3]–[9]. But there are still unknowns. Like, which is the exact role of each morphogen? Are there more types of neurons that follow the Hox-gene guided patterning? To which extend DV, and AP patterning influence each other? Which are the human-specific characteristics during the spinal cord patterning? To answer these questions and more, we need more complex models of the embryonic spinal cord than the ones that have been reported.

The spinal cord development and patterning can be studied using *in-vitro* models. Which, in contrast to animal models, allow to recapitulate species-specific differences. But, by using the traditional 2D in vitro culture systems of human stem cells, cell behaviour is

different than in the real 3D environment. Moreover, it is not possible to generate tissue-specific cell types.

Organoids, which have become easier to culture in recent years, are a promising alternative tool to study development. An organoid is a 3D multicellular tissue that is capable of recapitulating key features of development, such as tissue-specific cell types and architecture [10].

For example, Nakano et all. generated human retinal organoids from human embryonic stem cells (ESC), containing tissue-specific cell types as rods and cones, organized forming a multi-layered tissue. They used them to test the differences between human and mouse tissue morphogenesis and timing, by comparison with mouse retinal organoids [18].

Protocols for developing organoids to study different organs such as retina, gut, and kidney, among others, have so far been established [10]. In contrast, SCOs still lack characterization [19], only a few protocols have been published in the last three years [5] [6][8].

The generation of SCOs was first accomplished by Ogura et al. In 2018. In their report, they presented their 3D spinal cord induction condition (3-DiSC), which was designed by modifying a previously described protocol for in vitro spinal motor neuron induction. The 3-DiSC allowed them to develop a dorsal spinal cord tissue from human induced pluripotent stem cells (iPSCs), with four different types of dorsal interneurons (dI1, dI2, dI3, and dI4/6). Also, they proved that their tissue can be dorsalized by BMP4 treatment, and, by activating the Shh signalling, intermediate and ventral spinal-cord like tissues could be obtained [8].

In 2019, Duval et al. published two protocols for developing SCOs exhibiting dorsal interneurons from mouse ESCs and human iPSCs. Their study also confirmed that the BMP signalling pathway orchestrates the patterning of the dorsal neural tube [6].

Both protocols rely on treatments based on baths of patterning factors [5]. Although such type of treatments has allowed creating SCOs that recapitulate the major features of the organogenesis and disease phenotypes [20], they cannot direct cell differentiation in a spatial continuum [5].

Microfluidic devices can be used to recreate *in-vivo* concentration gradients [11], hence they can be used to overcome this problem and mimic the spinal cord more closely.

While alternative methods to develop these gradients have been proposed, microfluidic technology presents several advantages that make it more suitable in terms of predictability, reproducibility, biocompatibility, and cost [11].

Firstly, as microfluidic technology implies working on a relatively small scale, it allows designing high-resolution gradients, with a quick dynamic response and long-term stability. Also, use low amounts of reagents is possible, reducing the cost of its acquisition. Secondary, microfluidic devices are well suited for biological applications, as there are biocompatible materials that can be used for such application. Thirdly, microfluidic devices fabrication methods, such as soft-lithography or 3D printing, add flexibility and reduce the cost of the production process [11].

In 2019, Hor et al. took advantage of microfluidic device technology to culture SCOs. They designed a microfluidic device called microhexagon interlace for the generation of versatile and fine gradients (microHIVE), which allowed them to mimic the gradient of growth factors that induces the anterior-posterior patterning of the spinal motor neurons. Inside the microHIVE platform, they directed the differentiation from human iPSC into motor neurons, and they obtained, as a result, a patterned tissue with a progression of RNA and protein signatures characteristic of the lumbar, thoracic, and brachial regions of the spinal cord [5].

However, we still lack an *in-vitro* model capable of recapitulating completely and simultaneously the DV and AP patterning of the human embryonic spinal cord. The solution studied in this thesis, which takes advantage of both organoid and microfluidic device technology, have the potential to achieve this type of complexity.

Chapter 3

Materials and Methods

3.1. Microfluidic Device

The microfluidic device used is like the one published by Salmon et. Al [21] designed to vascularize organoids but adapted to generate an antiparallel concentration gradient instead. The previous design had a chamber to culture organoids, and two channels on both sides of the chamber connected to it by a grove. To vascularise the organoid in culture, endothelial cells and pericytes were perfused into the channels, so from there, they could reach the organoid inside the chamber spreading through the grove.

The adapted version has different inlets and outlets for each channel, instead of a common one, so the pattering factors can be different on each side of the chamber. Also, the culturing chamber has a square shape instead of circular, so the gradient is formed faster and more homogeneously, and the channels and the chamber are connected by windows instead of a groove in the bottom, so the surface of contact with the channels is bigger (Figure 6 A).
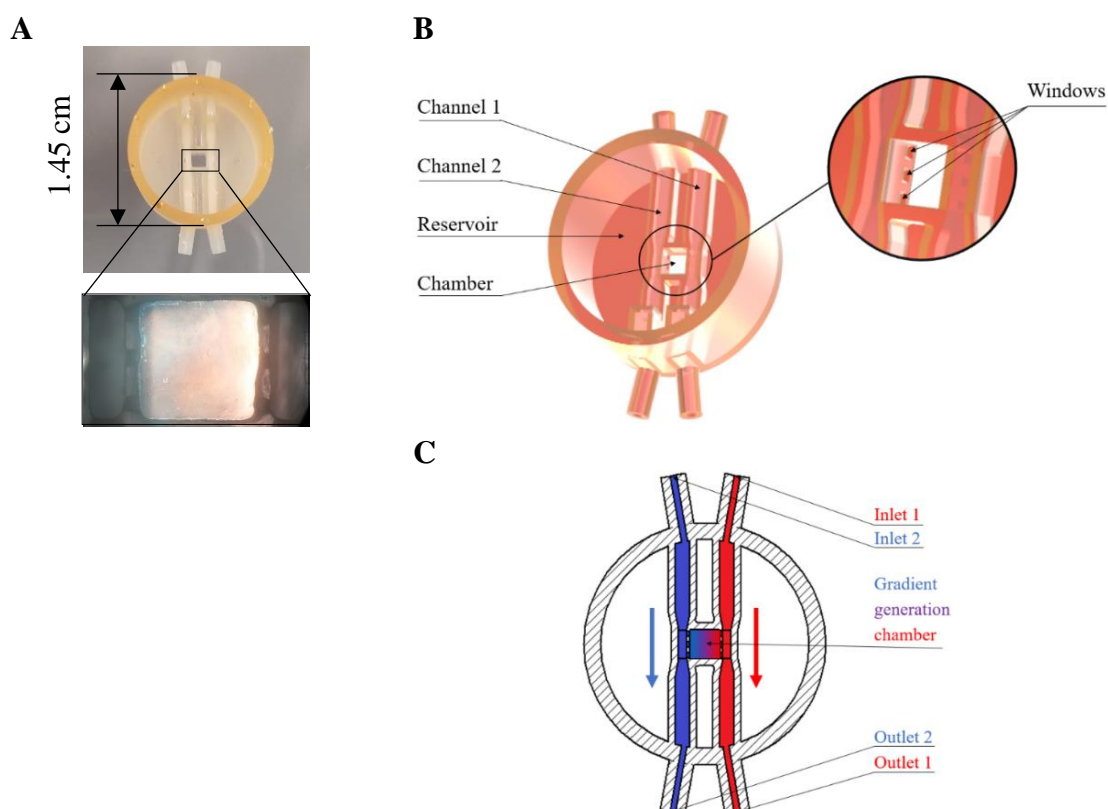
Figure 6.- The microfluidic device. (A) Real image of the microfluidic device, with an amplification of the gradient generation chamber. (B) Rendered 3D model of the microfluidic device with the two channels, the reservoir, the gradient generation chamber and the windows indicated. (C) Scheme of a section of the microfluidic device showing the antiparallel concentration gradient formed inside the chamber after the stabilization time. The blue and red arrows indicate the direction of the flow of the two liquids, that go from the inlets to the outlets of the channels.

The microfluidic device is 20.40 mm long, 14.50 mm wide and 7.00 mm high; and the chamber where the concentration gradient is formed is 1.74 mm long, 1.75 mm wide and 1.70 mm high. The two channels, located on each side of the chamber, are connected to the chamber by 3 windows, respectively. Also, on top of the chamber, there is a reservoir intended to contain media during culture experiments (Figure 6 B).

To generate the antiparallel concentration gradient, the two channels must be perfused, in the same direction and an uninterrupted manner, by two liquids with fixed concentrations of two different molecules. Also, the gradient generation chamber must be filled with hydrogel. Thanks to the windows, the liquids are in contact with the hydrogel and the molecules can diffuse through them. Once the stabilization time is reached, the antiparallel concentration gradient is completely formed inside the chamber (Figure 6 C).

Fabrication Process

The microfluidic device was designed using computer-aided design (CAD) software (Solid Edge) and fabricated by stereolithography (Form2, Formlabs). The printing preparation software utilized was PreForm and the printing parameters are shown in **Error! Reference source not found.**. The material is a certified biocompatible resin (Dental SG Resin, Formlabs) according to EN-ISO 10993-1:2009/ AC:2010. Moreover, it has been proved to be convenient for organ-on-chip applications, as it supports long term cell growth and the optical background is low [22] (Figure 7 A).

After printing, the microfluidic device is cleaned with isopropyl alcohol (ChemLab) and dried using a nitrogen pump (Figure 7 B). Then, a glass cover-slip is glued to the bottom of the device with a 5.6 µL of a clear and USP Class VI biocompatible adhesive (NOA 86, Norland Optical) (Figure 7 C). Once the coverslip is placed, the microfluidic device is cured for 2 min under UV light at room temperature and, subsequently, at 60°C for 2 h (Form Cure, Formlabs) (Figure 7 D).

To improve the biocompatibility of the microfluidic device, it is submerged in isopropyl alcohol for 6 days, replacing it each 2 days. At the end of the treatment, it is rinsed with Disinfectol (Chem-Lab) and Milli-Q (Millipore) and stored before using it (Figure 7 E).

Before using the microfluidic device, it is sterilized under UV for 30 min together with the other components that must be assembled: the platform, the lid, and the tubes, and the reservoirs. The platform is made of PLA and fabricated by fusion deposition modelling (FDM). The lid is a plexiglass lamina of 21x23x23 cm, cut using a laser cutter. The small ones are cut to measure 1 mm, and the large ones to measure 5 mm (Tygon S3™ E-3603, ACF00001, Saint-Gobain Performance Plastics). Lastly, the reservoirs are print and pre-processed in the same way as the microfluidic device but without the step of placing the cover-slip. Once the sterilization time is reached, all the components are assembled and the whole set is sterilized again under UV 30 min more (Figure 7 F).

Finally, on day 3, just before perfusing the channels with SAG, the tubing is connected to the microfluidic devices are placed in series, one after the other (Figure 7 G).
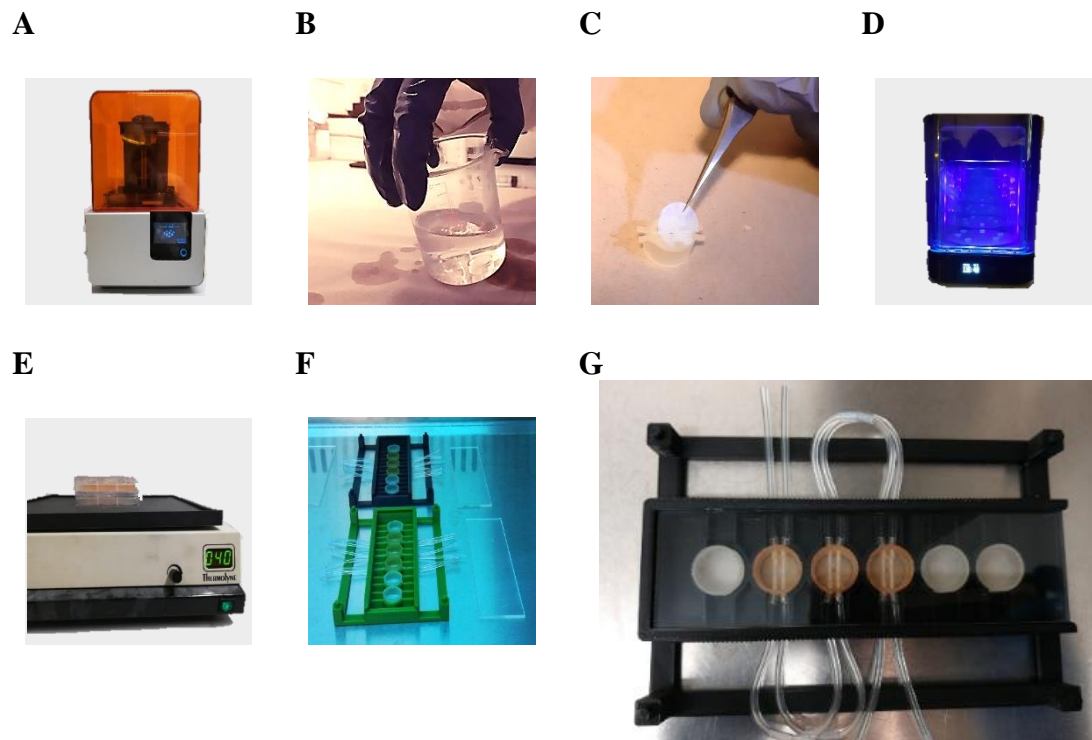
Figure 7.- Process to fabricate the microfluidic devices. (A) The microfluidic devices are 3D printed with a biocompatible resin. (B) After printed, the devices are cleaned with IPA. (C) A glass coverslip is glued on the bottom of the microfluidic devices. (D) The devices are cured under UV. (E) The microfluidic devices are treated with IPA. (F) The platform, the lid, the tubbing, the reservoir, and the microfluidic devices are sterilized under UV, ensembled and sterilized again. (G) Final assembly with the microfluidic devices placed in series connected by the tubing.

3.1. Organoids Culture

Human iPSC lines

The human iPSC lines used were hiPSC PAX3-mVenus/dox-H2B-mTurquoise2 (Received from Leiden UMC), and ZO1 hiPSC line (Mono-alleillic mEGFP - Tagged TJP1 WTC hPSC Line, Coriell Institute for Medical Research).

Culture mediums

The medium used to maintain hiPSC in culture was Essential 8 Flex Medium Kit (E8F) (ThermoFisher Scientific) supplemented with 1% of Penicillin Streptomycin (GIBCO)

The medium use to maintain the hNTO in culture was neural differentiation medium, which was a mixture of neurobasal medium (GIBCO) and DMEM/F12 (GIBCO) in a 1:1 relation, supplemented with 1% of N2 (GIBCO), 2% of B-27 (GIBCO), 1 mM of Sodium Pyruvate MEM (GIBCO), 1 mM of Glutamax (GIBCO), 1 mM of Non-essential amino acids (GIBCO), and 2% of Penicillin Streptomycin (GIBCO).

Human iPSCs culture

hPSCs were cultured in 6 well plates coated with Matrigel until a 60-70% confluence. Cells were passaged by treating them with Dispase (Sigma) at 37°C for 3-4 min. After that, cells were washed twice with PBS, 1 mL of E8F was added, and the colonies were scraped and agitated with a pipettor. Cells were passaged in a 1:8 ratio and incubated at

37°C in 2 mL of E8F supplemented with 10 μM of Y-27632 Rock inhibitor (RI) (Hellobio). After 24 h, the medium was replaced by 2 mL of E8F, and cells were keep incubated. The medium was replaced again each 48 h, if necessary, until the colonies reached the desired confluence of 60-70% to be passed again or 70-80% to be cultured as hNTOs.

To visualize the reporter of hiPSC PAX3-mVenus/dox-H2B-mTurquoise2, E8F was supplemented with 1 mg/mL of Doxcycyclin (DOX) (Sigma). To change the concentration, DOX was also applied at 0.5 mg/mL, 0.25 mg/mL, 0.125 mg/mL, 0.167 mg/mL, 0.1 mg/mL, and 0.083 mg/mL.

nd-PEG-A hydrogel preparation

To prepare the nd-PEG-A hydrogel, milli-Q water, 10X Buffer and nd-PEG were mixed in advance and kept at room temperature until hiPSC were ready to be embedded. Once ready, laminin (BD) and 10X FXIII were added, directly followed by the addition of the cells (Table 1).

Table 1.- Percentage of each component in the hydrogel mix.

Component	Percentage
Milli-Q	37.5 %
10X Buffer	10 %
nd-PEG-A	22.5 %
Laminin	10 %
Cells	10 %
10X FXIII	10 %

The preparation of the nd-PEG-A hydrogel components can be found in [12].

Human NTOs culture in nd-PEG-A

hiPSCs were kept in culture until a confluence of 70-80%. First, they were washed twice with PBS. Then, 1 mL of TrypLE Express (GIBCO) was added for 3 min at 37°C to dissociated them into single cells. After, 5 mL of DMEM/F-12 media were added, and cells were counted. The rest of the cells were centrifuged for 3 min at 300 RCF, then, the supernatant was discarded, and the pellet was resuspended in n2b27 media to obtain a cell density of 3 M per mL. After that, cells were added to a previously prepared nd-PEG-A mix to constitute 10% of the final volume. The mix was loaded into the microfluidic device chambers and the wells of the plate, forming droplets of 6 μL and 4 μL, respectively. The volume for the droplets in the device changed between experiments to 8 μL and 7.5 μL. Subsequently, the plates and the devices were spined up and down until the gelation time. Once the hydrogel reached the gelation time, which can be observed as it is when the hydrogel form fibrous structures, 20 min more of waiting time at room temperature ensured complete gelation. Then, 350 μL and 200 μL of n2b27 supplemented with both 10 μM of RI and 1 mg/mL of DOX, were added to the devices and the plates, respectively. From then on, cells were incubated at 37°C. The media was replaced with n2b27 after 24 h. After 72 hours, it was replaced again with n2b27 medium supplemented with 250 nM of retinoic acid (RA) (Stemcell Technologies) and 1 mg/mL of DOX. The media of the plates, and the group of devices where all the treatment was applied directly

on top, the media was also supplemented with 1 μM of smoothened agonist (SAG) (Stemcell Technologies). In the case of the rest of the devices, DMEM/F-12 supplemented with 4 μM of SAG was perfused through one of the channels using a syringe pump settled to produce a flow of 7.5 μL/min. After 72 h more, the medium was replaced with n2b27 supplemented with 1 mg/mL of DOX, and the perfusion was stopped. Then, the media was refreshed every two days until day 11.

To extend the RI treatment, cells were left with the n2b27 supplemented with RI during the first 72 h, without replacing the media. To avoid using DOX, all the protocol were the same but without supplementing the media with 1 mg/mL of DOX.

Immunohistochemistry of the hNTOs

They were fixed using 4 % paraformaldehyde (Sigma-Aldrich) for 1 h and then washed thrice with PBS, at intervals of 15-30 minutes. Blocking solution was added for 1 hour. Blocking solution was made with 0.3% Triton X (PanREAC AppliChem) and 0.5% BSA solution (Sigma-Aldrich). Hoechst was used to visualize nuclei. The devices were incubated overnight at 4°C with Hoechst, followed by washing thrice at intervals of 15-30 minutes.

Image Acquisition

Live images were taken with an inverted microscope (EVOS, Invitrogen) using 4x and 10 x air objective and the bright field. Fluorescence images were obtained using an inverted microscope (Zeiss Axio Observer Z1; Carl Zeiss MicroImaging) equipped with a Colibri LED light source and a 10x air objective.

Chapter 4

Results

4.1. Culturing hNTOs within the microfluidic device

The experiment aimed to evaluate if hNTOs could grow healthy within the microfluidic device, by comparing them with the control, hNTOs cultured in a 96 well plate.

During the experiment, the N2B27 media was supplemented with DOX to visualize the nuclear reporter of the cell line hiPSC PAX3-mVenus/dox-H2B-mTurquoise2. Moreover, during the first 24 h, it was also supplemented with RI (Figure 8 A).

The culture was stopped on day 3 because the hNTO in the microfluidic device were not growing properly. They were considered unhealthy for three reasons. Firstly, they had an irregular shape, whereas the ones of the control were circular. Secondly, they had zones with dead cells, which can be seen under the microscope as darker points. Thirdly, the hNTO of the microfluidic device were smaller than the ones in the control (Figure 8 B).

We primarily detected four problems that could have affected its development. Firstly, in some microfluidic devices, bubbles were formed on top of the chamber (Figure 8 C). Secondly, in the bottom of some devices and the control, a monolayer of cells was formed (Figure 8 D). Thirdly, a maroon layer appeared covering the top of the hydrogel of some microfluidic devices (Figure 8 E). Lastly, DOX could have affected the survival of the cells.
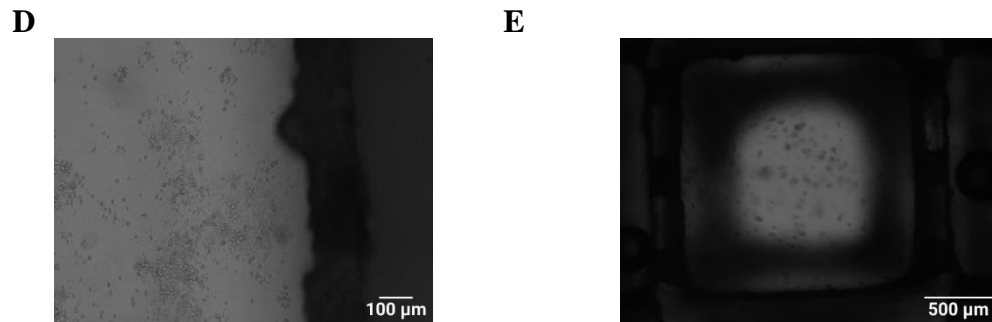
D   **E**
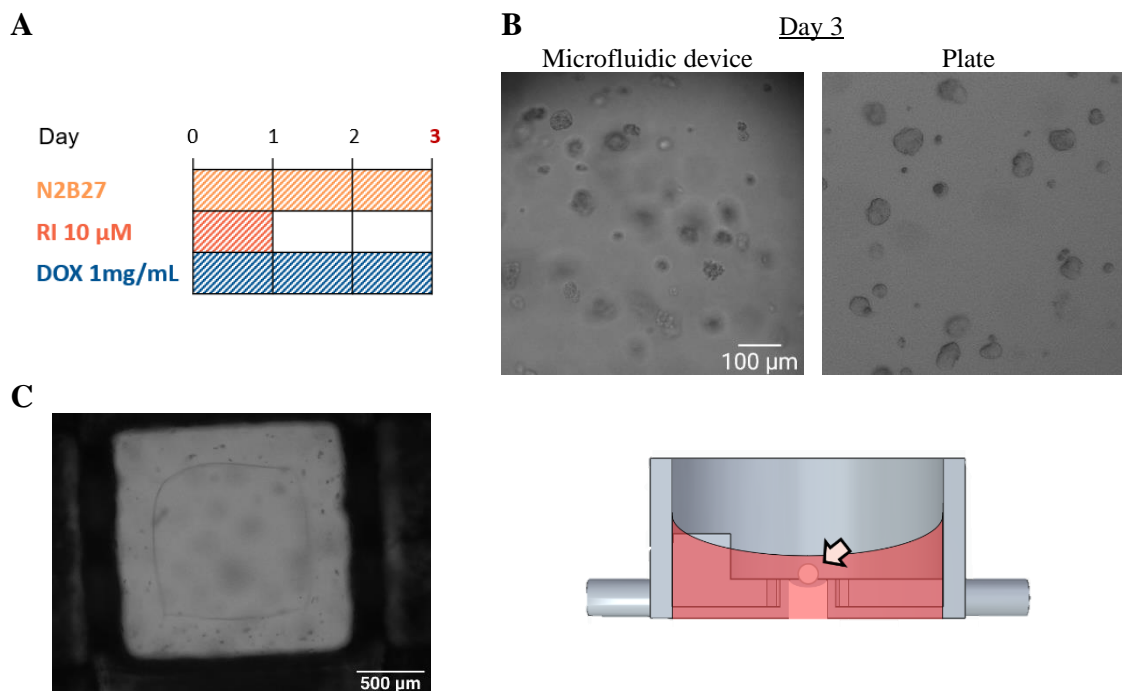
Figure 8.- Development of the hNTOs inside the microfluidic device. (A) Schematic of the followed protocol (B) At day 3, the organoids cultured in the microfluidic device are less healthy compared to the ones in the control. (C) The hydrogel does not fill all the chamber; thus, bubbles are trapped on top of it. (D) A dark layer covers the surface of the hydrogel. (E) The hNTOs fall to the bottom of the chamber forming a monolayer.

Bubbles were trapped on the top of the chamber

In some microfluidic devices, the bubbles present in the media were trapped on top of the hydrogel because the amount of hydrogel loaded inside the chamber (6 µL) was not enough to cover it to the top. The hypothesis was confirmed by seeing with the microscope a square mark on top of the hydrogel. This issue was a problem because the hydrogel changes its properties if it is in contact with air, thus it could affect the growth of the organoids.

The proposed solution to avoid this problem was to load the chamber with 8 µL instead of 6 µL of hydrogel.

A monolayer of cells was formed on the bottom of the hydrogel

In some devices and some wells of the control plate, hNTOs were falling to the bottom of hydrogel, forming a monolayer of cells. The issue of the monolayer was already seen in previous experiments in which the hNTOs were cultured in plates, and it is known that it occurs when the hydrogel is degrading because the media is added too early. Thus, the cause of having a monolayer was that the waiting time before adding the media was not enough.

The proposed solution was to be stricter with the timing to assure complete gelation of the hydrogel.

A maroon layer appeared on top of the hydrogel

An unexpected maroon layer appeared in the top of the hydrogel in some of the microfluidic devices, but not in the control. The apparition of this layer could not only have affected the growth of the hNTO, as the diffusion of the media through the hydrogel could be reduced, but also it impeded to take proper images of the organoids under the microscope, as it was opaque.

To understand why this maroon layer was forming, it was characterized. Firstly, by observing it under the microscope, it was seen that its texture was like dust (Figure 9 A). Moreover, to see how it evolved, some microfluidic devices were kept in culture for two

more days, until day 5. The result of this test showed that the layer was expanding and becoming thicker over time (Figure 9 B).
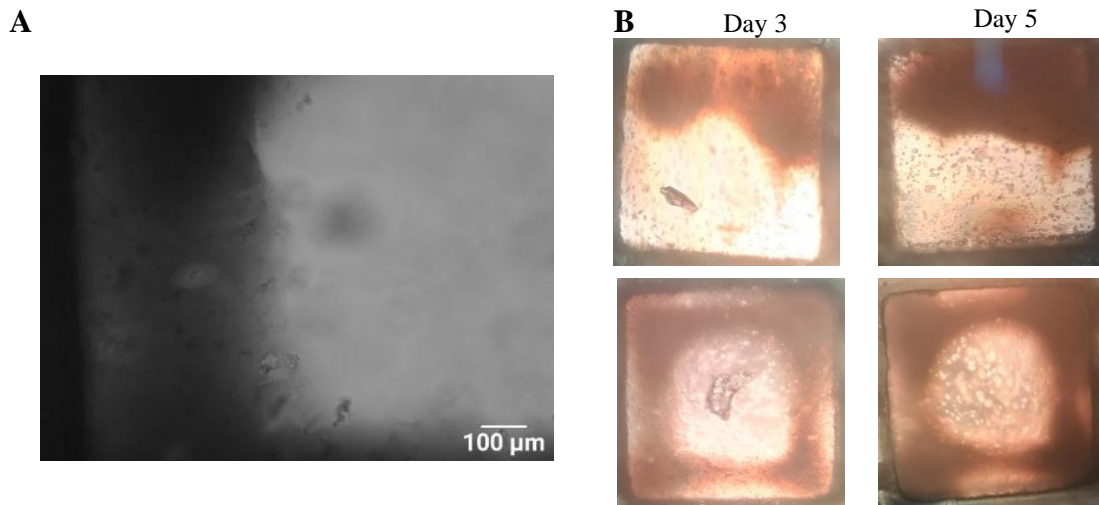

Figure 9.- Layer on top of the hydrogel in the microfluidic device analysed in detail. (A) The texture of the layer was like dust. (B) The layer expanded and become thicker over time.

Because of its texture, its colour, and the fact that the layer grew over time; it was deduced that it was made of media components that were deposited on top of the hydrogel induced by evaporation.

The proposed solution was to add reservoirs filled with ultrapure water (Milli-Q, Millipore Corporation) next to the microfluidic devices (Supplementary figure 2). Thereby, the relative humidity inside the microfluidic device was increased, and the evaporation of the media was prevented.

DOX could affect the survival of the cells

Finally, we noticed that the hiPSC in culture were not as healthy as normal before starting the experiment. This could have affected the development of the hNTOs. The difference compared to previous experiments was that the media was supplemented with DOX.

Thus, it was deduced that DOX was affecting their health. To check the hypothesis, an experiment was carried out. hiPSC were cultured at the same time with different concentrations of DOX. In the end, the results showed that DOX was not affecting the development of the hiPSC, as cells with treatment looked as healthy as the cells of the control, without treatment (Supplementary figure 1).

Regardless, it was decided to avoid adding DOX until the hNTOs were growing in the devices as healthy as in the plate. Thereby, fewer variables were introduced in the experiment.

Proposed improvements

Altogether, to solve the four detected problems, the proposed improvements were to load the chamber with 8 µL, respect strictly the timing during the gelation of the hydrogel, add reservoirs filled with ultrapure water next to the devices, and avoid using DOX (

Table **2**).

Table 2.- First proposed improvements regarding the detected problems.

PROBLEMS	SOLUTIONS
The chamber is not filled with 6 µL of hydrogel.	Increase the amount of hydrogel to 8 µL.
The hNTO fall to the bottom of the chamber creating a monolayer of cells.	Assure that the hydrogel is gelated by strictly respecting the timing.
It appears a maroon layer on top of the hydrogel.	Reduce evaporation by adding reservoirs filled with water.
DOX can affect the proper development of the hNTO.	Avoid using DOX until the hNTOs develop as in the control.

4.2. First optimization of the hNTOs culturing protocol

To evaluate if, after the corrections, it was possible to grow healthy hNTO within the microfluidic device, hNTOs were cultured again.

The set-up was the same, except from using DOX and that, from day 3 to day 5, hNTOs were treated with RA and SAG. For the treatment, the microfluidic devices were split into two groups. One group was treated by applying both RA and SAG directly in the media, like the control. Instead, the media of the other group was only supplemented with RA. And the SAG treatment was applied by perfusing one of the two channels with DMEM/F-12 with SAG, creating a concentration gradient inside the chamber (Figure 10 A).

Between day 3 and day 5, hNTOs stopped growing regardless they were in the microfluidic device or the control (Figure 10 B). Thus, there were still errors in the methodology.

The problems that we detected were that, firstly, at the start of the experiment cells were keep more than 1 h outside the incubator. Secondly, the hydrogel of some of the microfluidic devices flowed into the channels. Finally, the maroon layer was still appearing on top of the hydrogel.
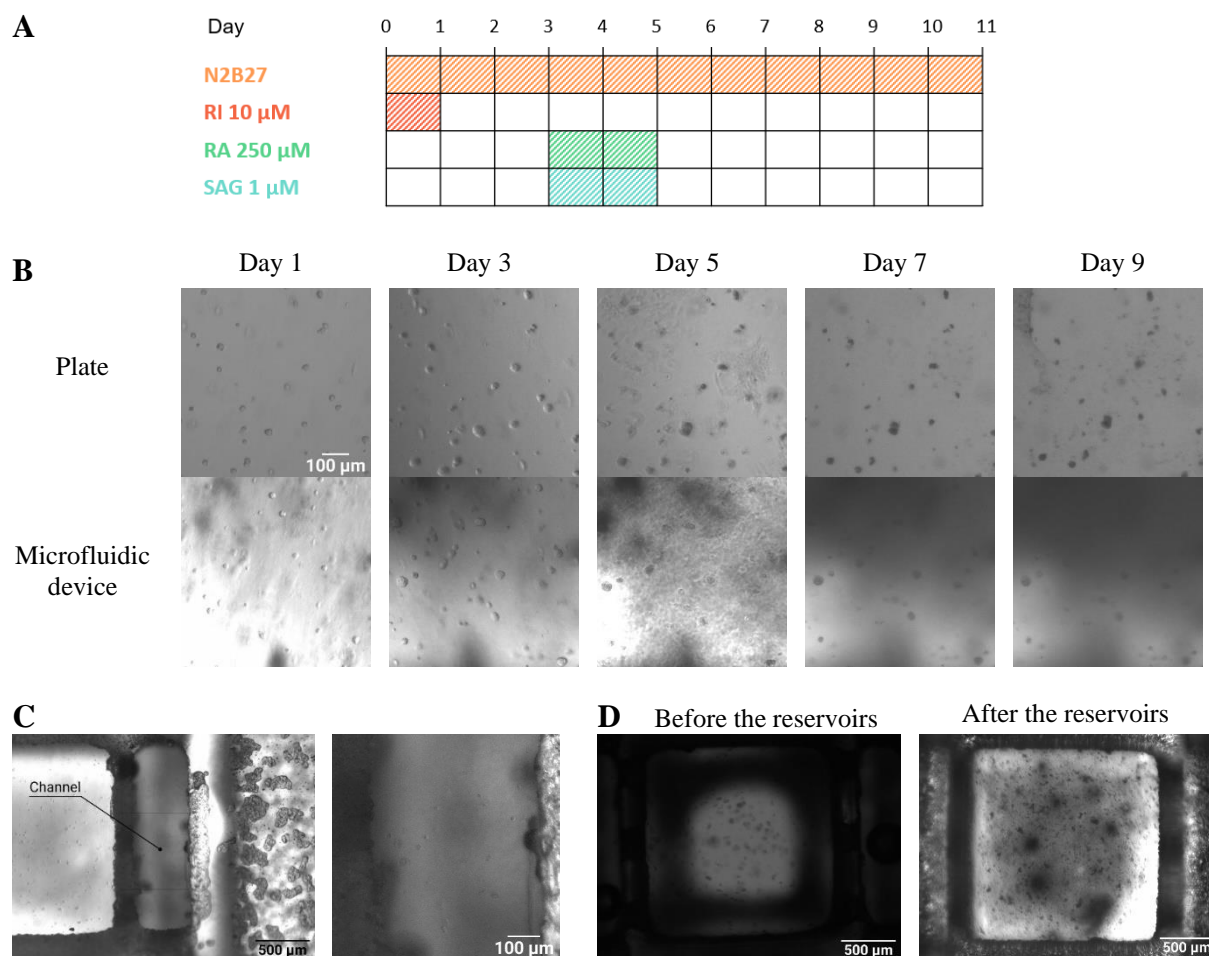
Figure 10.- Development of the hNTOs inside the microfluidic device after the first corrections. (A) Schematic of the followed protocol. (B) The hNTOs stopped growing after day 3, regardless of if they were in the microfluidic devices or the plate. (C) Some microfluidic devices had their channel blocked by the hydrogel. (D) The maroon layer on top of the hydrogel was less abundant but it was still present.

Improving loading speed of chips with cells and survival

On day 0, cells were more than 1 h outside the incubator. Being at room temperature for this amount of time could have affected the survival of the cells.

To avoid this issue, a detailed protocol with all the steps to culture the hNTOs and load the devices at day 0, and its corresponding timing was prepared (Supplementary table 2).

Moreover, to increase the survival ratio the RI treatment was extended until day 3.

Hydrogel blocked the channels of the devices

This time the chamber was filled. By contrast, some of the microfluidic devices had their channel trapped because the hydrogel went through the windows into the channels. Thereby, 8 µL was an excessive volume of hydrogel.

To find the optimal amount of hydrogel to use in the chips, we tested different volumes (7 µL and 7.5 µL). In none of the conditions, channels were trapped. As we wanted to use the maximum amount of hydrogel without blocking the channel, we continued with 7.5 µL.

24

Debris still visible in the microfluidic device

Even if the maroon layer was thinner, it was still present. As we had already reduced evaporation, but the level of media was still decreasing over time, we deduced that the microfluidic devices were leaking.

The problem of leaking was already faced by other laboratory mates that were using similar microfluidic devices. Thus, we apply the same solution as they. We incorporate a checkpoint, just before using the microfluidic devices. In this checkpoint, the microfluidic devices were filled with water, and be lived overnight. Then, the ones with less volume of water were discarded and the others used for the experiment.

Proposed improvements

Altogether, the proposed improvements were to follow the prepared protocol at day 0 to control better the timing, extend the RI treatment until day 3, load the chamber with 7.5 µL of hydrogel, and check leaking before using the devices (Table 3).

Table 3.- Second proposed improvements regarding the detected problems.

PROBLEMS	SOLUTIONS
Cells are kept for more than 1 hour outside the incubator at the beginning of the experiment.	Prepare a protocol to define better the timing of each step and extend the RI treatment until day 3.
Some of the microfluidic devices had their channels blocked by hydrogel.	Change from 8 µL to 7.5 µL of hydrogel to avoid overfilling the chamber.
The maroon layer on top of the hydrogel is less abundant but is still there.	Add a checkpoint to discard the microfluidic devices that were leaking.

4.2. Second optimization of the hNTOs culturing protocol

To evaluate if the second corrections were enough to grow healthy hNTO within the microfluidic device, hNTOs were cultured again using the same set-up as the previous experiment (Figure 11 A).

This time, on day 5 the hNTOs cultured in one of the microfluidic devices were as healthy as the ones in the control. They had a comparable shape and size. We also compared them with the hNTOs of previous experiments and we could confirm that they were all similar. After day 5, the incubator was contaminated by fungus and the microfluidic devices get infected (Figure 11 B).

The problems that we detected were that the microfluidic devices were prone to get infections (Figure 11 C), there were devices with blocked channels and trapped bubble, and the media did not cover always all the hydrogel (Figure 11 D).
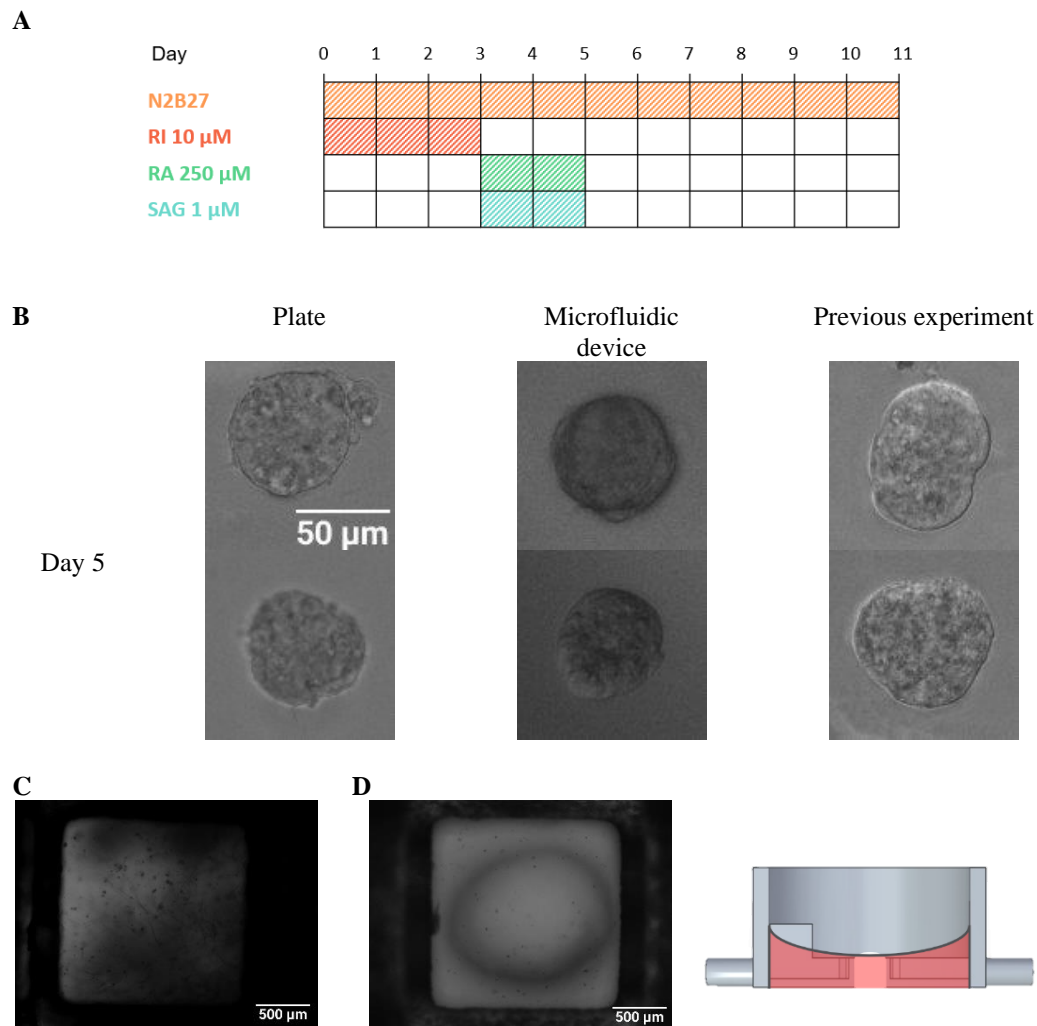
A

Day	0	1	2	3	4	5	6	7	8	9	10	11
N2B27												
RI 10 µM												
RA 250 µM												
SAG 1 µM												

B

	Plate	Microfluidic device	Previous experiment
Day 5		50 µm	

C   **D**

500 µm   500 µm

Figure 11.- Development of the hNTOs inside the microfluidic device after the second corrections. (A) Schematic of the followed protocol. (B) At day 5, in one of the microfluidic devices there were as healthy organoids as in the control. They were all circular and had a proper size, compared to previous experiments. (C) Microfluidic devices are more likely to get infections than the control. Fungal infection is spreading over the hydrogel. (D) The media in the microfluidic devices sometimes does not cover completely the hydrogel.

The microfluidic devices were prone to get infections

When the incubator was contaminated with fungus, the microfluidic devices were infected but not the control plate. The first devices that were infected, and that transmitted the fungus to the contiguous devices, were the ones that were the media was overflowing and spreading by capillarity between the top of the device and the lid.

To avoid the microfluidic devices overflowing we proposed to change the size of the platform to increase the distance between the top of the device and the lid.

Moreover, both, the glue, and the resin resisted high temperatures. we proposed to autoclave the microfluidic devices to improve the sterilization process. Starting with standard values of 121 °C of temperature and 2 bar of pressure for 15 min [22], and correcting them if necessary.

Channels blocked by hydrogel and bubbles

By using 7.5 µL of hydrogel, in some of the devices the chamber was still not covered with hydrogel while, in others, the hydrogel was flowing into the channels. Thus, there was no volume at which we could avoid both problems.

The proposed solution was to use 7 µL, as was the volume that was used to characterize the gradient inside the device and remove the bubbles that could be formed inside.

The media did not cover completely the hydrogel

The media of one of the microfluidic devices was not covering completely the hydrogel, even if the reservoirs had been added to reduce evaporation and the devices had been checked before using it to assure that it did not lick.

Thereby, we decided to increase the high of the device to make it able to contain 500 µL of media, the same as a well of a 24 well plate. The proposed solution was to increase the heigh of both, the platform and the device, 2 mm which was enough to contain 500 µL and served to increase the distance between the top of the media and the lid.

The maroon layer is not caused by media components

In Figure 11 D even if the media did not cover the hydrogel there were no traces of the maroon layer seen before. Thus, the maroon layer was not made of media components that were deposited on top of the hydrogel induced by evaporation.

To check if instead it was formed by dead cells, we stain the maroon layer with Hoechst. The result was that it was not, as there was no signal (Figure 12).
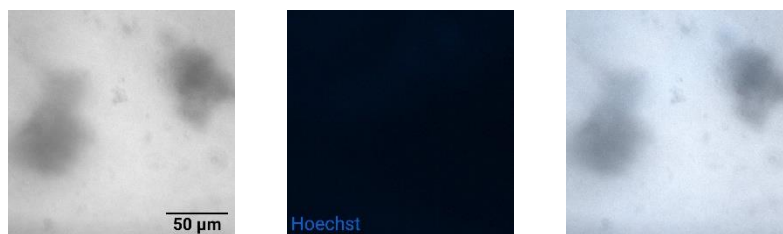

Figure 12.- There maroon layer is not formed by dead cells. The left image shows a part of the maroon layer in bright field, the image in the middle shows that there is no signal of Hoechst, and the image on the right is a composite of both.

The proposed solution was to evaluate in the next experiments two more hypotheses. First, if it was made by particles of the diluted painting of the pipettes, as we were using glass pipettes with IPA during the IPA treatment of the devices of the first experiments. Secondly, if it appeared because we take too long loading the devices, as during this time the hydrogel could have dried out and changed its properties.

Proposed improvements

Altogether, the proposed solutions were to autoclave the microfluidic devices, load the chamber of the devices with 7 µL of hydrogel and remove, if necessary, the formed bubbles, and increase the high of the devices and the platform 2 mm (Table 4).

Table 4.- Third proposed improvements regarding the detected problems.

PROBLEMS	SOLUTIONS
Microfluidic devices are more likely to get infections than plates.	Increase the distance between the media and the top of the lid. Autoclave the microfluidic devices.
Some of the microfluidic devices have their channels blocked by hydrogel and, in others, bubbles are trapped.	Change from 7.5 µL to 7 µL and remove the bubbles.
The label of media in the microfluidic device does not cover the hydrogel.	Increase the high of the microfluidic devices, and the platform 2 mm.

Chapter 5

Conclusion

Laboratory researcher skills

During the thesis, I acquired the skills of a laboratory researcher, and I learnt the protocols of the LBM necessary to fabricate the microfluidic device and to be able to generate hNTOs, and I used this knowledge to culture hNTOs within the microfluidic device.

Evaluation and optimization of the biocompatibility of microfluidic devices

We also evaluated the biocompatibility of the microfluidic device to generate neural tube organoids. The human neural tube organoids did no grow equally when compared to the control. Also, a few practical issues were identified when using the devices in the incubator, such as evaporation and higher infection chance.

Based on these results, we proposed different modifications for the protocol and the microfluidic device to improve the development and health of the hNTOs within the device. These were optimizing the amount of hydrogel in the chamber, improving the loading speed, and modifying the design and implementing water reservoirs to reduce evaporation. Moreover, we added a check-point to discard the devices that leaked (Table 2, Table 3)

Due to these improvements, we were able to culture healthy hNTOs until day 5. Unfortunately, the experiment had to be terminated due to a fungal infection. The proposed corrections were to a) autoclave the devices, to improve the sterilization process; b) increase the height of the platforms and the devices 2 mm.

In summary, we were able to modify the culture protocol to improve the health of the hNTOs within the microfluidic device and to make the process more robust and reliable. However, we could not evaluate if the formed gradient inside the device patterned the hNTOs matching the concentration of the SAG gradient in each position, because the hNTOs within the device were not healthy enough at day 11 to express the corresponding transcription factors.

Next steps and future work for the project

Apart from continuing working in the evaluation and optimization of the biocompatibility of the microfluidic devices, incorporating the proposed corrections and culturing hNTOs again, other future work should be considered.

Regarding the gradient, we were only using SAG. The final idea is to apply to the organoid an antiparallel gradient of SAG and BMP4. Thus, future work should be done to characterize the gradient formed in the microfluidic device in the case of a high molecular weight molecule as BMP4.

Moreover, we are culturing hNTOs from single cells. It is also possible to culture them from aggregates. This option is more adequate for our objective because to recapitulate

all the NP domains we require a bigger organoid covering all the chamber. Thus, using aggregates should be an important option to consider.

Additionally, we were working with hNTOs, instead of SCOs. To start working with SCOs, a different protocol has to be studied and implemented. Also, to be able to pattern the organoids in both the AP and DV axis, the protocol related to pattern the organoid in the AP axis should be studied.

Altogether, the project is on the right track to achieve the final objective to develop a spinal cord *in-vitro* model to study embryonic spinal cord development. But we must keep working on it and improving different aspects.

Appendices

Appendix A – Supplementary figures
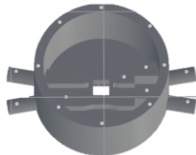
A

B
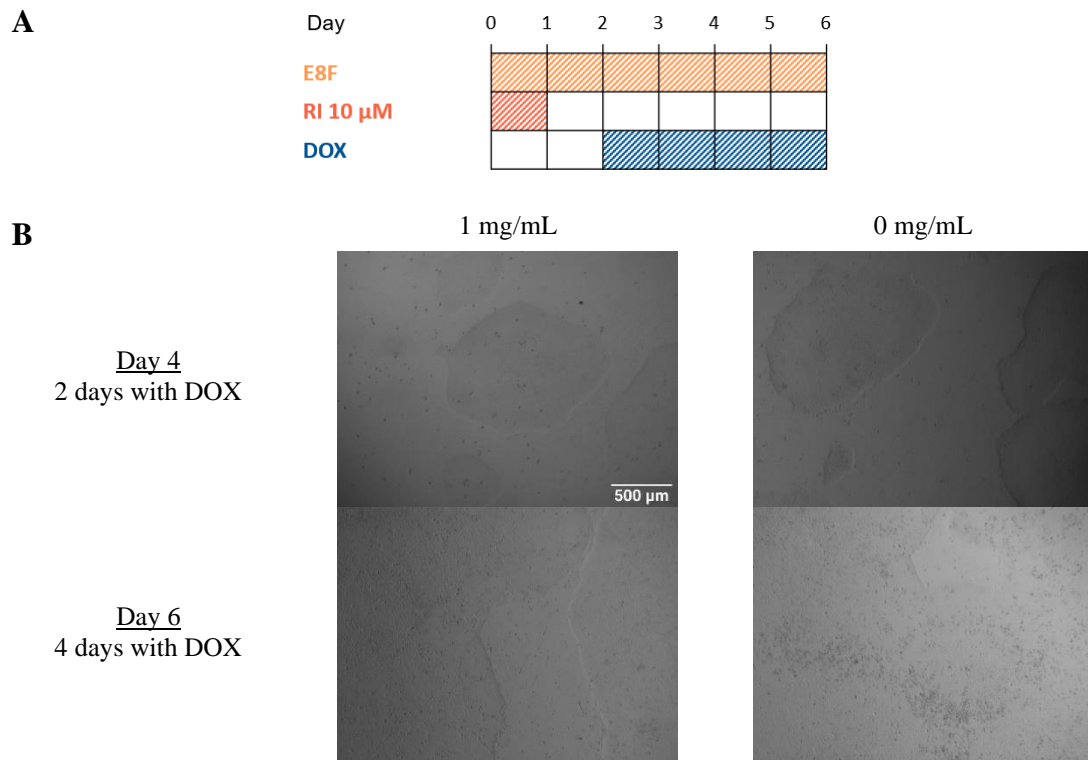
Supplementary figure 1.- DOX does not affect the development of the hiPSC. (A) Schematic of the followed protocol. (B) hiPSC develop as healthy after 2 and 4 days of treatment of DOX than the ones without treatment.
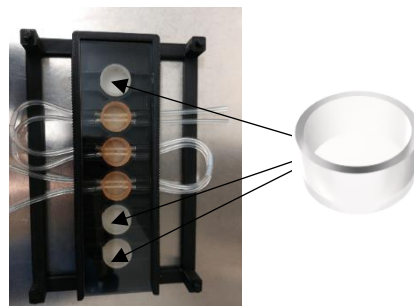
Supplementary figure 2.- Milli-Q reservoirs to reduce evaporation. The reservoir shown in the right is placed in the empty wells of the platform.

Appendix B – Supplementary tables

Supplementary table 1.- Parameters for 3D printing the microfluidic device.

GENERAL PARAMETERS	
Printer	Form2
Material	Dental SG
Layer thickness	0.05 mm
SUPPORT PARAMETERS	
Raft Type	Mini Raft
Density	1.00
Touchpoint Size	0.40 mm
Distribution	

Supplementary table 2.- Planification

STEP	TIME (min)
Remove the media + Wash with PBS	2
Add TryplE Express + Incubate + Check under the microscope	5
Transfer cells + Prepare the Neubauer cell counter chamber	2
Centrifugate + Cell counting	5
Discard media + Resuspend	4
Gel preparation + Loading	8
Waiting for complete gelation + Prepare media	20
Add media	2
Fill the tubes + Connect the tubes	7
Margin	5
TOTAL	60

Bibliography

[1]   A. Sagner and J. Briscoe, «Establishing neuronal diversity in the spinal cord: A time and a place», *Dev.*, vol. 146, num. 22, 2019, doi: 10.1242/dev.182154.

[2]   K. L. Tucker and T. Caspary, *Cilia and nervous system development and function*. Springer Netherlands, 2014.

[3]   F. Ulloa and J. Briscoe, «Morphogens and the control of cell proliferation and patterning in the spinal cord», *Cell Cycle*, vol. 6, num. 21. p. 2640-2649, 2007, doi: 10.4161/cc.6.21.4822.

[4]   F. Ille *et al.*, «Wnt/BMP signal integration regulates the balance between proliferation and differentiation of neuroepithelial cells in the dorsal spinal cord», *Dev. Biol.*, vol. 304, num. 1, p. 394-408, abr. 2007, doi: 10.1016/j.ydbio.2006.12.045.

[5]   G. S. Lim *et al.*, «Microhexagon gradient array directs spatial diversification of spinal motor neurons», *Theranostics*, vol. 9, num. 2, p. 311-323, 2019, doi: 10.7150/thno.29755.

[6]   N. Duval *et al.*, «Bmp4 patterns smad activity and generates stereotyped cell fate organization in spinal organoids», *Dev.*, vol. 146, num. 14, 2019, doi: 10.1242/dev.175430.

[7]   B. Leung and S. M. Shimeld, «Evolution of vertebrate spinal cord patterning», *Developmental Dynamics*, vol. 248, num. 11. John Wiley and Sons Inc., p. 1028-1043, nov. 10, 2019, doi: 10.1002/dvdy.77.

[8]   T. Ogura, H. Sakaguchi, S. Miyamoto, and J. Takahashi, «Three-dimensional induction of dorsal, intermediate and ventral spinal cord tissues from human pluripotent stem cells», *Dev.*, vol. 145, num. 16 Special Issue, 2018, doi: 10.1242/dev.162214.

[9]   Y. M. Elkouby and D. Frank, «Wnt/β-Catenin Signaling in Vertebrate Posterior Neural Development», *Colloq. Ser. Dev. Biol.*, vol. 1, num. 1, p. 1-79, gen. 2010, doi: 10.4199/C00015ED1V01Y201007DEB004.

[10]   M. A. Lancaster and J. A. Knoblich, «Organogenesisin a dish: Modeling development and disease using organoid technologies», *Science*, vol. 345, num. 6194. American Association for the Advancement of Science, jul. 18, 2014, doi: 10.1126/science.1247125.

[11]   X. Wang, Z. Liu, and Y. Pang, «Concentration gradient generation methods based on microfluidic systems», *RSC Advances*, vol. 7, num. 48. p. 29966-29984, 2017, doi: 10.1039/c7ra04494a.

[12]   A. R. A. Fattah *et al.*, «Actuation enhances patterning in human neural tube organoids», *bioRxiv*, 2020, doi: 10.1101/2020.09.22.308411.

[14]   *Clinical anatomy of the spine, spinal cord, and ANS*, 3rd ed. St. Louis: Elsevier, 2014.

[15]   J. S. Dasen and T. M. Jessell, «Chapter Six Hox Networks and the Origins of Motor

Neuron Diversity», *Current Topics in Developmental Biology*, vol. 88. Academic Press, p. 169-200, gen. 01, 2009, doi: 10.1016/S0070-2153(09)88006-X.

[16] H.-Y. Ko, *Management and Rehabilitation of Spinal Cord Injuries*. Springer Singapore, 2019.

[17] W. A. Alaynick, T. M. Jessell, i S. L. Pfaff, «SnapShot: Spinal cord development», *Cell*, vol. 146, núm. 1. p. 178.e1-178.e1, 2011, doi: 10.1016/j.cell.2011.06.038.

[18] T. Nakano *et al.*, «Self-formation of optic cups and storable stratified neural retina from human ESCs», *Cell Stem Cell*, vol. 10, núm. 6, p. 771-785, 2012, doi: 10.1016/j.stem.2012.05.009.

[19] R. Vieira De Sá, M. Cañizares Luna, and R. J. Pasterkamp, «Advances in Central Nervous System Organoids: A Focus on Organoid-Based Models for Motor Neuron Disease», *Tissue Engineering - Part C: Methods*, vol. 27, núm. 3. p. 213-224, 2021, doi: 10.1089/ten.tec.2020.0337.

[20] Winanto, Z. J. Khong, J. H. Hor, and S. Y. Ng, «Spinal cord organoids add an extra dimension to traditional motor neuron cultures», *Neural Regeneration Research*, vol. 14, núm. 9. Wolters Kluwer Medknow Publications, p. 1515-1516, set. 01, 2019, doi: 10.4103/1673-5374.255966.

[21] I. Salmon *et al.*, «Engineering neurovascular organoids with 3D printed microfluidic chips», *bioRxiv*, p. 1-22, 2021, doi: 10.1101/2021.01.09.425975.

[22] K. Piironen, M. Haapala, V. Talman, P. Järvinen, and T. Sikanen, «Cell adhesion and proliferation on common 3D printing materials used in stereolithography of microfluidic devices», *Lab Chip*, vol. 20, núm. 13, p. 2372-2382, jul. 2020, doi: 10.1039/d0lc00114g.